Heart and large vessel interaction in congenital heart disease, assessed by magnetic resonance imaging

Grotenhuis, H.B.

Heynric B. Grotenhuis
Albert de Roos
Jaap Ottenkamp
Paul H. Schoof
Hubert W. Vliegen
Lucia J.M. Kroft

chapter 10

MR Imaging of Right Ventricular Function after the Ross Procedure for Aortic Valve Replacement - Initial Experience.
Radiology. 2008; 246 (2): 394-400.

Abstract

Purpose: To prospectively assess right ventricular (RV) function after the Ross procedure by using magnetic resonance imaging (MRI).

Materials and Methods: The local ethics committee approved the study and informed consent was obtained from all participants prior to enrollment in the study. Seventeen patients (15 male, two female; mean age ± standard deviation, 19 years ± 3.9; imaging performed 8.3 years after surgery ± 3.2) and 17 matched controls (15 male, two female; mean age ± standard deviation, 20 years ± 3.9) were studied by using MRI. Standard velocity-encoded and multisection multiphase imaging sequences were used to assess homograft valve function, systolic and diastolic RV function, and RV mass. The two-tailed Mann-Whitney U test and the Spearman rank correlation coefficient were used for statistical analysis.

Results: Minor degrees of homograft stenosis (peak flow velocity between 1.5 and 3.0 m/s across the homograft valve) were found in 12 of 17 patients but not in controls ($P < 0.001$). A larger RV mass was present in Ross procedure patients than in controls (17.0 g/m^2 ± 4.8 vs 10.9 g/m^2 ± 5.6, $P = 0.004$). In addition, impaired diastolic RV function was found, as shown by a decreased mean tricuspid valve early filling phase-atrial contraction phase (E/A) peak flow velocity ratio (1.56 ± 0.75 vs 2.05 ± 0.58, $P = 0.03$). Peak velocity across the homograft valve correlated with RV mass ($r = 0.38$, $P = 0.03$) and tricuspid valve E/A peak flow velocity ratio ($r = 0.39$, $P = 0.02$). RV systolic function was normal in Ross procedure patients (mean RV ejection fraction, 52% ± 8 vs 51% ± 5; $P = 0.74$).

Conclusion: RV hypertrophy and RV diastolic dysfunction are frequently observed in patients after the Ross procedure, even in the absence of overt homograft stenosis. RV systolic function is still preserved.

Introduction

Aortic valve replacement, according to the Ross procedure, is frequently performed in the pediatric population (1,2). During this operation, the stenotic or regurgitant aortic valve is replaced by a pulmonary autograft, while a homograft valve is inserted in the pulmonary position (1). Potential advantages of this procedure are the use of the patient's own valve with favorable hemodynamic characteristics, avoidance of anticoagulant therapy, and the alleged growth potential of the autograft valve in children (2,3). Long-term survival is satisfactory, although frequent dilatation of the autograft in the aortic position and diminished left ventricular (LV) function have been reported (2-4).

The longevity of the homograft valve in pulmonary position is reported to be limited owing to frequent homograft stenosis: shrinkage of the homograft annulus occurs because of a postoperative immune-mediated response to the homograft, as well as calcification and thickening of the valve leaflets (2,3,5-10). As a result, homograft stenosis is the main cause for a reoperation after the Ross procedure, necessary in approximately 10% of all cases at long-term follow-up (2,3,10,11).

Little is known about the effect of early homograft stenosis on right ventricular (RV) function. Insight into this relationship is relevant as RV function has prognostic value concerning patient survival and exercise tolerance (12,13) and may contribute to optimal timing for replacement of a dysfunctioning homograft valve.

Echocardiography is a widely used imaging tool in clinical practice but has limitations in assessment of RV function owing to the complex RV geometry (12). Magnetic resonance imaging (MRI) has been established as an accurate noninvasive tool for the assessment of the pulmonary valve and RV function (14-16). To our knowledge, MRI has not previously been used to study the relationship between homograft valve function and systolic and diastolic RV function in patients after the Ross procedure.

We hypothesized that minor degrees of homograft stenosis occur frequently in patients after the Ross procedure and that the associated increased RV afterload may negatively affect RV function. Thus, the objective of our study was to prospectively assess RV function after the Ross procedure by using MRI.

Materials and Methods

Patients

The medical ethics committee of Leiden University Medical Center (Leiden, The Netherlands) approved the study and informed consent was obtained from all participants prior to their enrollment in the study. Seventeen Ross procedure patients (mean age ± standard deviation, 19 years ± 3.9; imaging performed 8.3 years after surgery ± 3.2) and 17 age- and gender-matched healthy controls were prospectively studied with MRI at our institution (Table 1).

Tabel 1. Characteristics of patients and controls.

Characteristics	patients (n = 17)	controls (n = 17)
male / female	15 / 2	15 / 2
range of age at MRI by birth sex (years)	12.9 - 25.1/13.8 - 20.6	12.8 - 25.8/14.1 - 21.2
age at Ross procedure (years) *	10.8 ± 5.2	
interval between the operation and the MRI (years) *	8.3 ± 3.2	
height (cm) *	174 ± 13	179 ± 10
weight (kg) *	65 ± 15	72 ± 16
Body Surface Area (m^2) * and †	1.8 ± 0.3	1.9 ± 0.3

* Data are mean ± standard deviation.
† According to the Mosteller formula: √ (height (cm) × weight (kg) / 3600).
Abbreviations: MRI = magnetic resonance imaging.

Ross procedure patients were recruited from our local database of 53 Ross procedure patients. The inclusion criterion was aortic valve previously corrected with the Ross procedure. Exclusion criteria included age younger than 12 years and older than 25 years (n = 25), a Konno extension to the Ross procedure (i.e., relief of LV outflow obstruction by using septal patch insertion, n = 3), repeat operation and/or intervention in the homograft area between the Ross procedure and MR investigation (n = 1) and general contraindications to a cardiovascular MR examination. Seven patients declined to participate for personal reasons.

Age- and gender-matched healthy controls were selected from our database of individuals with a harmless heart murmur in which congenital cardiac disease had been excluded in the past by physical examination and echocardiography. Patient characteristics and functional status, as classified on the basis of the New York Heart Association functional class standards, were obtained from the patient records (Table 1). All patients were identified as New York Heart Association functional class I, without using medication.

LV function analysis of the patient group used in this study and their matched healthy controls have previously been described (4).

Operative technique

The Ross procedure was performed in patients with aortic valve disease (median age at surgery, 10.8 years; mean age, 10.8 years ± 5.2) by using cardiopulmonary bypass with moderate hypothermia by 2 surgeons (P.H.S. and a nonauthor, with 11 years experience each with the Ross procedure) (3). In all patients the pulmonary autograft was implanted by using the root replacement technique (17). Reinforcement of proximal and distal suture lines with a strip of autologous pericardium was used in all patients except 1. Autograft harvesting was performed after aortic cross-clamping. The RV outflow tract was reconstructed with a cryopreserved pulmonary homograft valve in all patients. Associated procedures during the Ross procedure were enucleation or resection of a discrete subaortic stenosis in 3 patients and ventricular septal defect closure in 2.

MRI

MRI studies were performed with a 1.5-T system (NT 15 Gyroscan Intera; Philips Medical Systems, The Netherlands).

Flow dynamics across the homograft valve were assessed by using velocity-encoded MRI just distal to the homograft valve. In the control group, velocity-encoded MRI was performed just distal to the pulmonary valve (15). Imaging parameters were: repetition time in ms / echo time in ms, 8.6 / 5.3; field of view, 400 mm; flip angle, 20°; voxel size, 2.34 × 2.61 × 8.00 mm. The sequence was encoded for a through-plane velocity of up to 150 cm/s. In case of aliasing owing to flow velocity exceeding 150 cm/s, the imaging was repeated with through-plane velocity encoding up to 300 cm/s. Temporal resolution was 25.6 ms.

Systolic biventricular function was assessed with a steady-state free precession cine sequence in the short-axis plane by using breath holds (15). Imaging parameters were: repetition time in ms / echo time in ms, 3.2 / 1.6; field of view, 400 mm; flip angle, 70°; voxel size, 1.6 × 1.6 × 8.00 mm; and no section gap (14,15).

Diastolic RV function was assessed by using velocity-encoded MRI across the tricuspid valve (15,18). Imaging parameters were: repetition time in ms / echo time in ms, 9.4 / 6; flip angle, 20°; voxel size, 2.34 × 2.61 × 8.00 mm. The sequence was encoded for a through-plane velocity of up to 100 cm/s. Temporal resolution was 25.6 ms.

Postprocessing

All images were quantitatively analyzed on a workstation with a Pentium 4 processor (Intel, USA).

Systolic RV and LV function were analyzed with the software package MASS (Medis, The Netherlands) (14,15). Biventricular end-diastolic volume (EDV) and end-systolic volume (ESV) were assessed by drawing the RV and LV endocardial contours at end-diastole and end-systole in all sections, as described previously (14). At end-diastole, epicardial borders of the RV free wall were drawn to obtain the RV mass (15). The interventricular septum was included in the LV analysis. Indexation was performed according to the Mosteller formula (BSA = √ (height

(cm) × weight (kg) / 3600)), where BSA is the body surface area in square meters. The following parameters were then determined: EDV, ESV, stroke volume, ejection fraction (EF) and ventricular mass (14).

Flow velocity-encoded MR data were analyzed with the software package FLOW (Medis, The Netherlands) (15,16). Flow curves were obtained with this method for homograft or pulmonary artery flow during the cardiac cycle. Contours were drawn for the homograft (patients) or pulmonary artery (controls) lumen, and flow data were subsequently obtained from the velocity data of each voxel in all phases. Peak flow velocity was determined with a time-velocity analysis that revealed the voxel with maximum peak flow throughout the cardiac cycle. Peak flow velocity across the homograft valve or pulmonary valve was considered substantially increased if maximum blood flow velocity (V_{max}) exceeded 1.5 m/s (19).

Pressure gradients across the homograft and pulmonary valves were subsequently calculated by using the simplified Bernoulli equation: $\Delta P = 4V^2$, where ΔP is the pressure gradient across the valve (mm of mercury), 4 is the estimated loss coefficient, and V is the peak flow velocity (m/s) (20). The regurgitant fraction was calculated with the following formula: regurgitant flow / systolic forward flow × 100%, where flow is measured in mm. Valve regurgitation was considered substantial if the regurgitant fraction exceeded 5% of the systolic forward flow (14).

Analysis of diastolic RV function by measuring flow through the tricuspid valve was performed by using the same method (14). Peak flow velocity curves were obtained for calculation of early filling phase, atrial contraction phase and early filling phase / atrial contraction phase (E/A) peak flow velocity ratios. Calculation of mean deceleration gradients of the early filling phase was used for analysis of the early filling phase slopes. The times of the early filling phase, atrial contraction phase and diastasis were also measured (16).

The manual drawing of all MR contours and analysis of the other results were performed by one researcher (H.B.G., with 3 years experience in cardiac MRI) and were subsequently checked by a radiologist (L.J.M.K., with 9 years experience in cardiac MRI), who was unaware of the patient's conditions.

Statistical analysis

Statistical analysis was performed by using software (SPSS for Windows, version 12.0.1; SPSS, USA). All data are expressed as mean value ± 1 standard deviation, unless stated otherwise. The Mann-Whitney U test was used to express differences in variables between the patients and controls. Correlation between variables was expressed with the Spearman rank correlation coefficient. Statistical significance was indicated by a P value of less than 0.05.

Results

Homograft and pulmonary valve characteristics

In 12 (82%) of 17 Ross procedure patients, the homograft valve V_{max} exceeded 1.5 m/s (compared with none from the control group), indicating minor degrees of homograft stenosis (Figure 1, Table 2). Calculated pressure gradients derived from these peak flow velocities were 16.8 mm Hg ± 9.0 in patients (range: 4.3 - 36.0 mm Hg) and 4.0 mm Hg ± 1.5 in controls (range: 2.1 - 7.6 mm Hg; $P < 0.001$). No regurgitant flow across the homograft valve in any patient or the pulmonary valve in any control was present.

Figure 1.

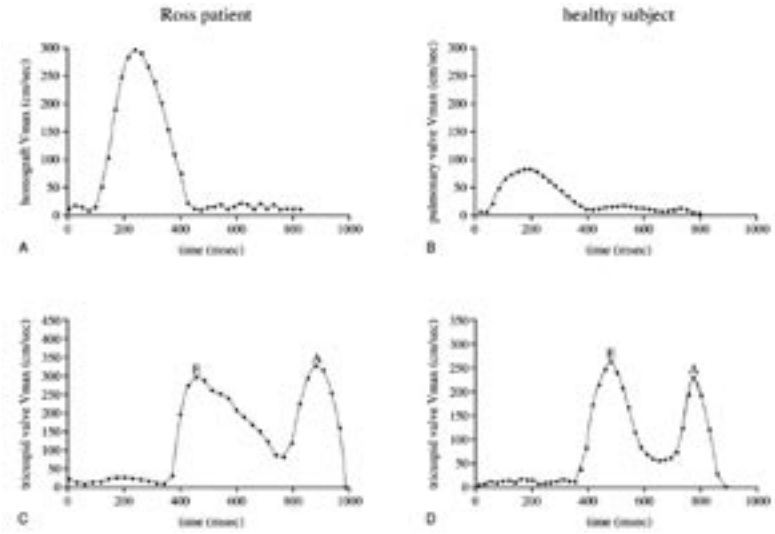

Figure 1a-d. Graphs show peak flow velocity curves across pulmonary homograft valve in **(a)** Ross patient and **(b)** control. Time between surgery and MR was 7.5 years. Note markedly increased peak flow velocity during systole in Ross patient (maximum velocity, 300 cm/s), indicating homograft stenosis (derived pressure gradient, 36 mm Hg). RV inflow curves across tricuspid valve in **(c)** Ross patient and **(d)** control. Biphasic inflow pattern has early filling and atrial contraction phase peaks. Note decreased tricuspid valve E/A peak flow velocity ratio and decreased mean deceleration gradient in early filling phase in Ross patient as compared with control, indicating delayed RV relaxation.

Table 2. Results in Ross procedure Patients and Controls.

parameters	patients	controls	P value
V_{max} (m/s)*	1.97 ± 0.56	0.99 ± 0.18	< 0.001
pressure gradient (mm Hg)*	16.8 ± 9.0	4.0 ± 1.5	< 0.001
RV EF (%)	52 ± 8	51 ± 5	0.74
RV SV (ml/m^2)	54 ± 8	52 ± 8	0.84
RV EDV (ml/m^2)	106 ± 13	107 ± 16	0.64
RV ESV (ml/m^2)	53 ± 14	52 ± 8	0.69
RV mass (g/m^2)	17.0 ± 4.8	11.7 ± 4.9	0.004
TV E/A peak-flow ratio	1.56 ± 0.75	2.05 ± 0.58	0.03
TV mean dec gradient of E phase (l/s^2)	-2.67 ± 1.09	-3.05 ± 1.03	0.39
TV diastasis time (ms)	46 ± 54	74 ± 89	0.55
LV EF (%)	50 ± 6	57 ± 5	0.001
LV EDV (ml/m^2)	67 ± 16	56 ± 11	0.03
LV ESV (ml/m^2)	34 ± 8	33 ± 4	0.99
LV mass (g/m^2)	33.0 ± 8.6	28.4 ± 5.9	0.04

Note: data are expressed as mean ± standard deviation.
* homograft and pulmonary artery in patients and controls, respectively.
Abbreviations: V_{max} = maximum velocity, RV = right ventricle; EF = ejection fraction; SV = stroke volume indexed for Body Surface Area; EDV = end-diastolic volume indexed for Body Surface Area; ESV = end-systolic volume indexed for Body Surface Area; TV = tricuspid valve; E = early filling phase; A = atrial contraction phase; dec = deceleration; LV = left ventricle.

Biventricular Function

Systolic function - expressed as RV EF and RV stroke volume - was not found to be different between Ross procedure patients and controls (Table 2). Also, RV dimensions (EDV and ESV) were not found to be different between the two groups (Table 2). Mean RV mass of the Ross patient group was significantly larger than in controls (Table 2). In addition, a significantly lower mean tricuspid valve E/A peak flow velocity ratio in Ross procedure patients as compared with the controls reflected a delayed RV relaxation (Figure 1, Table 2). Mean deceleration gradients of the early filling phase, and the times of the early filling phase, atrial contraction phase, and diastasis were not significantly different between the two groups (Table 2). In the Ross patient group, higher peak flow velocities across the homograft valve were significantly correlated with RV mass ($r = 0.38$, $P = 0.03$) (Figure 2) and with the E/A peak flow velocity ratio across the tricuspid valve ($r = 0.39$, $P = 0.02$) (Figure 3).

Figure 2.

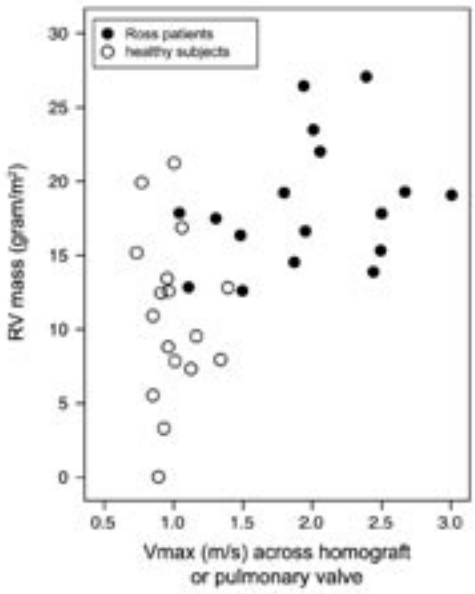

Figure 3.

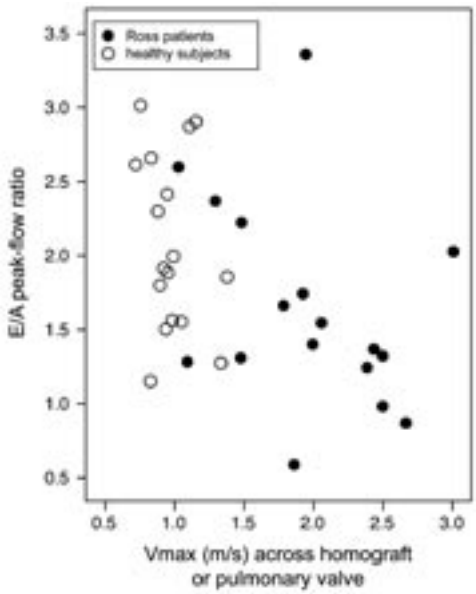

Figure 2. Scatterplot shows distribution of relationship between peak flow velocity across homograft or pulmonary valve vs indexed RV mass in Ross procedure patients and controls. Mild degrees of homograft stenosis represented by higher peak flow velocities across homograft valve were responsible for RV hypertrophy as compensatory mechanism owing to increased RV afterload.

Figure 3. Scatterplot shows distribution of relationship between peak flow velocity across homograft or pulmonary valve vs E/A peak flow ratio across tricuspid valve in Ross procedure patients and controls. Diastolic RV dysfunction in Ross group (lower mean tricuspid valve E/A peak flow velocity ratio) results from increased RV afterload and concomitant RV hypertrophy.

LV systolic function, expressed as LV EF, was diminished in the Ross procedure patients as compared with controls (Table 2). Mean LV EDV and LV mass were significantly larger in the Ross procedure patients as compared with controls (Table 2), while mean LV ESV was not significantly different between the two groups. RV EF and LV EF were not significantly correlated in the Ross patient group ($r = 0.21$, $P = 0.12$). In addition, LV mass was not significantly correlated with RV mass ($r = 0.28$, $P = 0.10$) or with peak flow velocity across the homograft valve ($r = 0.12$, $P = 0.48$).

Discussion

Our study findings revealed RV hypertrophy and diastolic dysfunction in patients after the Ross procedure, in the presence of mild degrees of homograft stenosis. Systolic RV function was preserved.

Ross procedure patients showed higher peak flow velocities across the homograft valve, with calculated pressure gradients up to 36 mm Hg reflecting mild degrees of homograft stenosis (19), whereas all values were below 8 mm Hg in our controls. Despite favorable survival rates and low incidence of reoperation when compared to other valve substitutes such as mechanical valves and xenografts, degeneration and calcification of the homograft valve can cause homograft stenosis (2,3,5-10).

Homograft valve regurgitation occurs only in a minority of cases (2,5), as is consistent with our data. Homograft stenosis is caused by an early postoperative immune-mediated response to the homograft that leads to shrinkage of the homograft annulus (2,3,5-10) and calcification and thickening of the valve leaflets (2,3,8,10). Stenosis predominantly occurs during the first 2 years after surgery (9,10), although others have reported progression at a later stage (2,3,5,6). A gradient exceeding 9 mm Hg at 1 year follow-up could be used to predict the late occurrence of homograft stenosis (10).

Other predictive variables for homograft valve durability are related to homograft antigenicity and to the size of the inserted homograft valve (6,10). Reduced viability of the donor cells within the homografts has been shown to be favorable; older donor age and a longer duration of graft cryopreservation were associated with a lower rate of homograft stenosis (6,10). Oversizing of the homograft by 2 - 3 mm facilitates homograft valve performance (6,10). Nevertheless, somatic outgrowth remains an important contributor to homograft valve failure in the pediatric population (2,10), as may have been the case in our patient group with a mean age at surgery of 10.8 years.

Systolic RV function was adequately preserved in our patients after the Ross procedure and all were identified as New York Heart Association functional class I. However, mean RV mass was significantly higher as compared with that in the controls, indicating RV hypertrophy in the Ross patient group. RV hypertrophy often occurs as a compensatory mechanism owing to increased RV afterload (21), which in our study was related to mild degrees of homograft stenosis, as represented by higher peak flow velocities across the homograft valve.

As homograft stenosis can progress over time owing to continuing degeneration of the homograft valve or somatic outgrowth, RV hypertrophy may increase during follow-up. In addition, higher LV mass may have contributed to RV hypertrophy (22), although LV mass and RV mass were not significantly correlated in our Ross patient group. Also, a direct correlation was

found between homograft peak flow velocity and RV mass, but not with LV mass, illustrating the functional effect of homograft stenosis on the RV.

Impaired RV diastolic function was reflected by a significantly lower mean tricuspid valve E/A peak flow velocity ratio as compared with those values in controls. RV diastolic dysfunction is a consequence of hypertrophy owing to stiffening of the myocardium and may precede RV systolic dysfunction (21). Impaired diastolic function is a primary cause in 30 - 40% of patients with congestive heart failure (18,21) and is associated with diminished exercise performance (13). As physiologic loss of elastic myocardial properties and increasing ventricular mass during lifetime contribute to diastolic dysfunction (18,21), current RV diastolic dysfunction in our Ross patient group might pose a future risk for progressive RV dysfunction. Further studies are needed to address the long-term effects of our results.

Homograft replacement is suggested from a pressure gradient of 50 mm Hg or more or when signs of RV dysfunction are present (3). Therefore, serial follow-up assessment of homograft valve and RV function with noninvasive imaging techniques is useful for early detection of homograft valve dysfunction, which may facilitate selecting patients for possible reoperation. In addition, exercise testing may help assess the functional implications of homograft and RV dysfunction. Although transthoracic echocardiography is the most commonly used imaging technique, it has limitations such as a reduced acoustic window with increased patient age and difficulty helping to assess RV function, owing to the complex RV geometry.

MRI overcomes these limitations, as accurate assessment of homograft valve function and systolic and diastolic RV function can be achieved in one imaging session with low inter- and intraobserver variability (15,23,24). MRI should primarily be used for patient follow-up owing to its good reproducibility (15,23,24), as identification of patients with RV dysfunction remains difficult considering the variation in RV function parameters as depicted in Figures 2 and 3 and the fact that clear cut-off values for RV dysfunction are still lacking. Although MRI will not replace transthoracic echocardiography as the imaging technique of choice owing to higher costs and reduced availability, it should be considered when echocardiographic imaging is difficult or when actual homograft replacement is considered.

Our study had limitations. We used a limited number of patients and controls, although the low inter- and intraobserver variability of cardiac MRI allowed for relatively small sample sizes (25). No preoperative or follow-up measurements were available in our observational study, so progression of findings could not be documented. Further research is required to define cut-off values of homograft valve and RV function for optimal timing of homograft replacement in patients after the Ross procedure.

In conclusion, cardiac MRI revealed mild degrees of homograft stenosis in patients after the Ross procedure, as evidenced by higher peak flow velocities across the homograft valve. Hemodynamic consequences were RV hypertrophy and diastolic dysfunction, whereas systolic

RV function was preserved. Our study showed the feasibility of MRI as an integrated imaging tool to monitor homograft valve and RV function in patients after the Ross procedure, which may facilitate the early detection of homograft valve dysfunction. MRI may facilitate better selection of patients who need reoperation after the Ross procedure for homograft valve dysfunction.

References

1. Ross DN. Replacement of aortic and mitral valves with a pulmonary autograft. Lancet. 1967; 2: 956-958.
2. Takkenberg JJ, Dossche KM, Hazekamp MG et al. Report of the Dutch experience with the Ross procedure in 343 patients. Eur J Cardiothorac Surg. 2002;22:70-7.
3. Bohm JO, Botha CA, Horke A et al. Is the Ross operation still an acceptable option in children and adolescents? Ann Thorac Surg. 2006;82:940-7.
4. Grotenhuis HB, Westenberg JJ, Doornbos J et al. Aortic root dysfunctioning and its effect on left ventricular function in Ross procedure patients assessed with magnetic resonance imaging. Am Heart J. 2006;152:975-8.
5. Gulbins H, Kreuzer E, Reichart B. Homografts: a review. Expert Rev Cardiovasc Ther. 2003;1:533-9.
6. Raanani E, Yau TM, David TE, Dellgren G, Sonnenberg BD, Omran A. Risk factors for late pulmonary homograft stenosis after the Ross procedure. Ann Thorac Surg. 2000;70:1953-7.
7. Sinzobahamvya N, Wetter J, Blaschczok HC, Cho MY, Brecher AM, Urban AE. The fate of small-diameter homografts in the pulmonary position. Ann Thorac Surg. 2001;72:2070-6.
8. Ward KE, Elkins RC, Overholt ED et al. Evaluation of cryopreserved homografts in the right ventricular outflow tract after the Ross procedure: intermediate-term follow up. J Heart Valve Dis. 1997;6:130-3.
9. Carr-White GS, Kilner PJ, Hon JK et al. Incidence, location, pathology, and significance of pulmonary homograft stenosis after the Ross operation. Circulation. 2001;104:I16-I20.
10. Feier H, Collart F, Ghez O et al. Risk factors, dynamics, and cutoff values for homograft stenosis after the Ross procedure. Ann Thorac Surg. 2005;79:1669-75.
11. Khambadkone S, Coats L, Taylor A et al. Percutaneous pulmonary valve implantation in humans: results in 59 consecutive patients. Circulation 2005;112:1189-97.
12. Carr-White GS, Kon M, Koh TW et al. Right ventricular function after pulmonary autograft replacement of the aortic valve. Circulation. 1999;100:II36-II41.
13. Singh GK, Greenberg SB, Yap YS, Delany DP, Keeton BR, Monro JL. Right ventricular function and exercise performance late after primary repair of tetralogy of Fallot with the transannular patch in infancy. Am J Cardiol. 1998;81:1378-82.
14. Van Straten A, Vliegen HW, Hazekamp MG et al. Right ventricular function after pulmonary valve replacement in patients with tetralogy of Fallot. Radiology. 2004;233:824-9.
15. van der Geest RJ, Reiber JH. Quantification in cardiac MRI. J Magn Reson Imaging. 1999;10:602-8.
16. Pluim BM, Lamb HJ, Kayser HW et al. Functional and metabolic evaluation of the athlete's heart by magnetic resonance imaging and dobutamine stress magnetic resonance spectroscopy. Circulation. 1998;97:666-72.
17. Stelzer P, Jones DJ, Elkins RC. Aortic root replacement with pulmonary autograft. Circulation. 1989;80:III209-III213.

18. Paelinck BP, Lamb HJ, Bax JJ, van der Wall EE, de Roos A. Assessment of diastolic function by cardiovascular magnetic resonance. Am Heart J. 2002;144:198-205.
19. Gutberlet M, Boeckel T, Hosten N et al. Arterial switch procedure for D-transposition of the great arteries: quantitative midterm evaluation of hemodynamic changes with cine MR imaging and phase-shift velocity mapping-initial experience. Radiology. 2000;214:467-75.
20. Oshinski JN, Parks WJ, Markou CP et al. Improved measurement of pressure gradients in aortic coarctation by magnetic resonance imaging. J Am Coll Cardiol. 1996;28:1818-26.
21. Mandinov L, Eberli FR, Seiler C, Hess OM. Diastolic heart failure. Cardiovasc Res. 2000;45:813-25.
22. Niezen RA, Helbing WA, van der Wall EE, van der Geest RJ, Rebergen SA, de Roos A. Biventricular systolic function and mass studied with MR imaging in children with pulmonary regurgitation after repair for tetralogy of Fallot. Radiology. 1996;201:135-40.
23. van der Geest RJ, de Roos A, van der Wall EE, Reiber JH. Quantitative analysis of cardiovascular MR images. Int J Card Imaging. 1997;13:247-58.
24. van der Geest RJ, Niezen RA, van der Wall EE et al. Automated measurement of volume flow in the ascending aorta using MR velocity maps: evaluation of inter- and intraobserver variability in healthy volunteers. J Comput Assist Tomogr. 1998;22:904-11.
25. Bellenger NG, Davies LC, Francis JM, Coats AJ, Pennell DJ. Reduction in sample size for studies of remodeling in heart failure by the use of cardiovascular magnetic resonance. J Cardiovasc Magn Reson. 2000;2:271-8.